Egyptian Geophysical Society
EGS Journal, Vol. 19, No. 1, 163-173 (2021)

USING RADIOELEMENTS COMPOSITE COLOUR TECHNIQUE FOR INTERPRETATION OF THE AIRBORNE GAMMA RAY SPECTROMETRIC DATA, WEST MALLAWI AREA, CENTRAL WESTERN DESERT, EGYPT

A.M.M. MOHAMED

Airborne Geophysics Dept., Exploration Division, Nuclear Material Authority,
P.O. Box 530, Maadi, Cairo, Egypt.

استخدام تقنية المركبات الأشعاعية الملونة لتفسير البيانات الإشعاعية الجوية ،

لمنطقة غرب ملوي ، وسط الصحراء الغربية ، مصر

الخلاصة: الهدف من هذه الدراسة هو البحث عن المعادن والمواد المشعة في منطقة الدراسة واستكشافها. تقع منطقة الدراسة غرب ملوي في وسط الصحراء الغربية لمصر، غرب نهر النيل. تهدف هذه الدراسة إلى تفسير أشعة جاما المحمولة جواً لإنشاء خريطة سطحية بناءً على وجهة نظر الإشعاع وتحديد المناطق الغنية بالمحتوى الإشعاعي ثم مقارنتها بالخريطة الجيولوجية. وتم عمل أيضا الصورة المركبة التي تجمع عنصر البوتاسيوم باللون الأزرق وعنصر اليورانيوم باللون الأحمر وعنصر الثوريوم باللون الأخضر والتي أظهرت أن الإشعاع العالي المستوى (المناطق المضيئة) في المنطقة الشمالية الشرقية من منطقة الدراسة. وتم إنشاء خريطة تقسيم المناطق عن طريق تقسيم منطقة الدراسة إلى مناطق بناءً على اختلاف اللون في الصورة المركبة. ثم تحديد الأماكن الأكثر سطوعًا (إشعاعا) من الصورة المركبة ثم تجميعها في خريطة واحدة وهي خريطة Radioelement Leads ثم إنتاج الصور المركبة بنسب عنصر إشعاعي اثنين وثلاثة لتقليل التأثيرات المزعجة وتباين الصورة ولتعزيز الاختلافات الدقيقة في تركيزات العناصر بسبب التغيرات الصخرية أو عمليات التغيير المرتبطة بالتمعدن. وتم حساب أيضا معدل التعرض للإشعاع في خريطة معدل التعرض لتوفير المعلومات الأساسية حول الخلفية الطبيعية التي يمكن استخدامها كمرجع لأي تغييرات محتملة في المستقبل. بالإضافة إلى ذلك ، تم حساب معدل الجرعة الإشعاعية للكشف عن درجة الخطر على البشرية والتأثيرات المختلفة على الأنسجة البيولوجية.

ABSTRACT: *The aim of this study is to search and explore for minerals and radioactive materials in the west Mallawi area, The study area is located in central Western Desert of Egypt, west of the Nile River. This study aims to interpret the airborne gamma rays to create a surface map based on the gamma radiation measurements to identify areas rich in radioactive content and compare them with the geological map. Subsequent analysis steps are applied to achieve our goal, which include elements maps (eU, eTh and K), which show that the major structural trend is the NW-SE, the composite image that collects eU (red), eTh (green), and K (blue) data, and then generating a zoning map by dividing the area into regions based on color difference in composite image. The brightest places were determined from the composite image and grouped into one map which is the Radioelement Leads Map. The two and three radioelement ratios composite images were produced to reduce the disturbing effects and contrast of the image and to enhance subtle variations in elemental concentrations due to lithological changes or alteration processes associated with mineralization, Ratio pattern maps (eU/eTh, eU/K and eTh/K) were constructed. Other maps were made to show sites of mineralization in the area, such as the (eTh*K)/eU ratio data that showed areas of high (eTh*K), the (eU*K)/eTh ratio data that showed areas of high (eU*K) and the (eU*eTh)/K ratio data that showed areas of high (eU*eTh).*

The rate of exposure to radiation was calculated and presented in an exposure rate map to provide basic information about the natural background that can be used as a reference for any possible changes in the future. In addition, the radiation dose rate was calculated to reveal the degree of danger to mankind and the various effects on biological tissus. Concerning the study area and its surroundings the mean natural radiation dose rates from the terrestrial gamma-radiation range from 0.0 to 0.5 mSv/y.

INTRODUCTION

West Mallawi area is located (Fig. 1) between latitude 27° 42′ to 27° 51′ N and longitude 29° 58′ to 30° 18′ E. It is Located on the western side of the Nile River at distance of about 50 Km west of Mallawi city. The study area.

TOPOGRAPHY

The elevation map of West Mallawi area (Fig. 2) shows clearly a northwest-southeast high topographic trends reaching in elevation 160m. The area is characterized by general slopping on both sides of this high topographic trend to the northeast and southwest areas, reaching elevation values of 78 and 117m above sea level respectively. Meanwhile, there are three hilly areas with elevations which range from 135 to 160m.

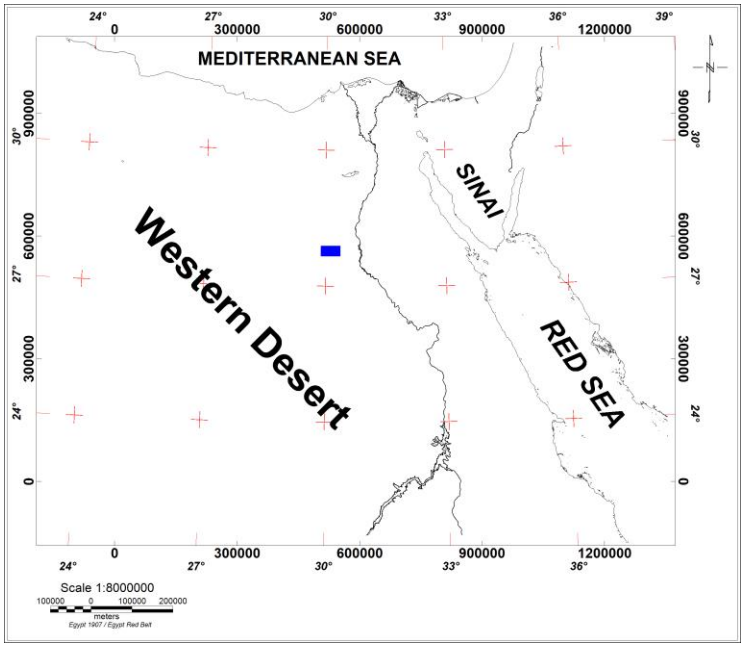

Fig. (1): Egypt Map Showing the Location of the West Mallawi Area, Western Desert, Egypt.

THE LANDSAT IMAGE

A figure (3) represents the false-colour Land Sat Satellite Multispectral Scanner (MSS) photomap of the study area published by the Egyptian Remote Sensing Center (Atlas, 1992). This photomap has been produced by the processing of the digital data acquired with resolution 82 x 57 meters restored to -50 x 50 meters.

Visual analysis of Landsat image (Atlas, 1992) was utilized for mapping and identification of the lineaments and litho-structural features associated with mineralization. The analysis revealed that the area was heavily structurally controled and have been subjected to various successive movements, since the late Cretaceous and early Tertiary. The predominant lineaments have NNW-SSE to NW-SE and NNE-SSW to NE-SW trends (Fig. 3). The NW-SE trend is common in all rock exposures of the area. In general, these lineaments are running conformably with the regional structural trends of the central Western Desert. They are, also, running conformably with the major structural trends of the area such as the elongation and stretching, the structural trends of the acidic and mafic dyke swarms.

GEOLOGIC MAP

The study area is characterized by three important tectonic events; regional uplifts during early and late Paleozoic, the separation of the Apulia micro-plate during Jurassic and the movement of the North African plate toward Europe during the late Cretaceous and early Tertiary. The structural elements of the Central Western Desert are the result of typical stable shelf tectonics. Faults, to a lesser extent and large scale gentle folds are reflected on the surface and these indicate differential block movements in the basement rocks. The surveyed area comprises the following stratigraphic units (Fig. 4): Mokattam Group Tems: Samalut Formation (Shallow marine limestone, middle Eocene) is presented in the middle south of the map, Temh: Mokattam Group, Hamra Formation Burrowed sandstone rocks (middle- upper Eocene) is present in the northwestern corner of the map, Abu Muharik Formation Tea: (continental to Littoral marine alternating clastics, siltstone, and reddish claystone siltymarl, upper Eocene) is occupying large part at the southwest of the map, Toq: Gebel Qatrani Formation (Littoral claystone siltymarl marl with Nummulites and white limestone, Oligocene) is occupying large part at the north of the map and Gravel Quaternary Qg: Oligocene to Pleistocene is present in the eastern side of the map.

AIM AND SCOPE OF WORK

1. The aim of this work is the exploration for mineralization and radioactive materials achieved through Processing of the spectrometric data using the most recent techniques and software package to produce the radioelement concentration maps of the study area.
2. Generation of Radioelements maps (K, eU and eTh) and composite image.
3. Generation of two elements ratio maps (eU/eTh, eU/K and eTh/K).
4. Generation of three elements ratio maps (eTh*K)/eU, (eU*K)/eTh, (eU*eTh)/K.
5. Generation of two/three radioelements ratio composite images.

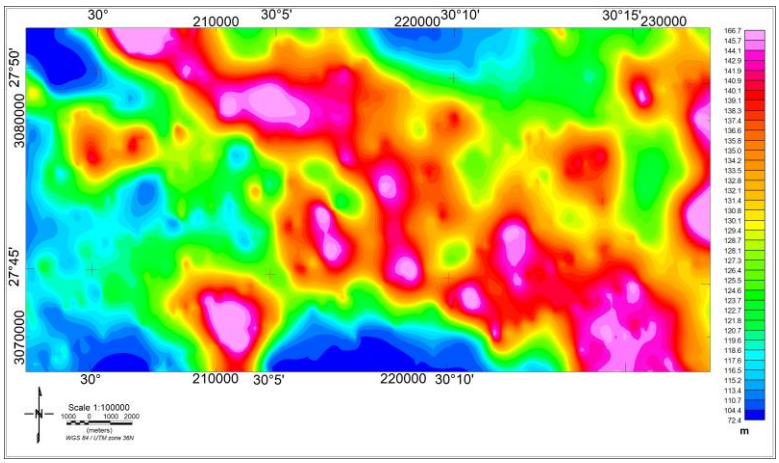

Fig. (2): The Elevation Map of the West Mallawi Area, Central Western Desert, Egypt.

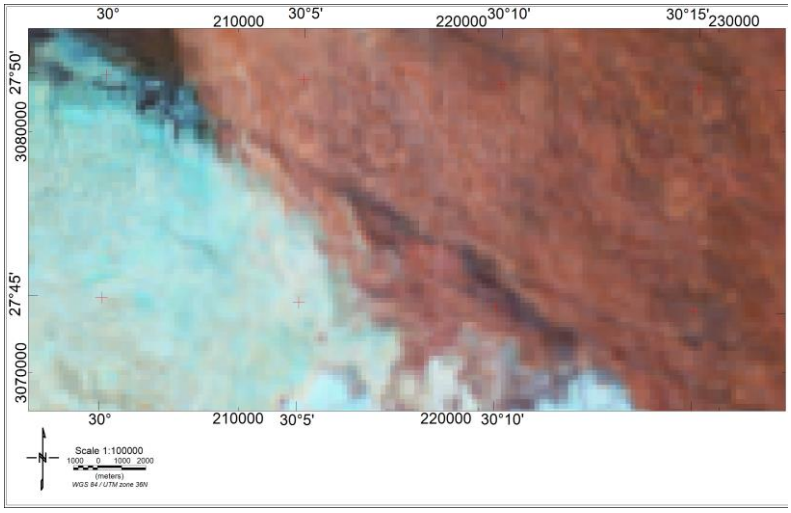

Fig. (3): False Colour Landsat MSS Image of the West Mallawi Area, Central Western Desert, Egypt.

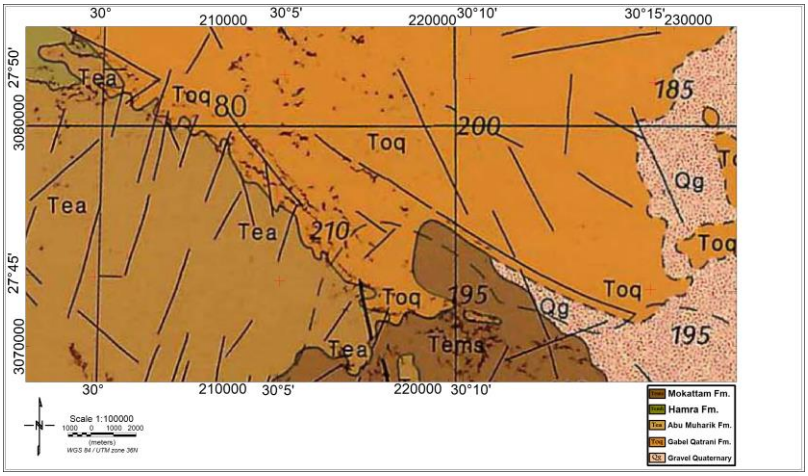

Fig. (4): The Geologic Map of the West Mallawi Area, Central Western Desert, Egypt (After Conoco, 1987).

6. Interpretation of the airborne spectrometric data to map surface geology and assessment of the radioactive mineral potentiality of the study area. The interpretation will be committed through applying ternary imaging technique.
7. Integration of the results obtained from the spectrometric interpretation to correlate the mapped geology, surface structure, radioelement concentration and environmental study.
8. Identification of anomalous zones of uranium, thorium and potassium concentrations if present.

the following processes:

Establishment of the radiation exposure rate to provide basic information of the natural background that can be used as a reference for any possible future variations. In addition, the radiation dose rate will be calculated to reveal the degree of the hazard on humanity and different effects on biological tissues.

DESCRIPTION OF GAMMA-RAY SPECTROMETRIC MAPS

The four parameters (variables) namely: total-count of the gamma radiation (TC, in µR/h) absolute concentrations of the three radioelements: potassium (K, in %), equivalent uranium (eU, in ppm) and equivalent thorium (eTh, in ppm) (Figs. 5, 6, 7 & 8) show relative variation of the gamma radiation. The three main radiometric elemental concentrations mainly reflect the lateral variation of surface elemental concentrations of different rock and soil types (Charbonneau et al, 1976).

The major trend that could be traced from the spectrometric maps (Figs. 5, 6, 7 & 8) is the NW-SE. The lowest level encountered in the four spectrometric maps is conjugated with the Abu Muharik Formation which is more or less having the same feature of very low radiometric effect. The Abu Muharik Formation is located in the southwestern parts of the study area. This level could be seen as blue color on the four maps and has values ranging between zero to17 µR/h in TC, zero to 1.2 ppm in eU, zero to1.5ppm in eTh, and 0 to 0.1% in K. The highest level of radiation is found in northeastern part, conjugated with the Gebel Qatrani Formation where the radiation has values ranging between 55 to 65 µR/h in TC, 3 to 5.2 ppm in eU, 7 to 9 ppm in eTh and 0.3 to 0.4 % in K.

on the TC map (Fig. 5) the highest value (65µR/h) is related to Gebel Qatrani Formation (Toq) and Gravel Formation (Qg). Also, in eU, eTh and K maps these two rock units give high values which reach 5, 9 ppm and 0.4 % respectively.

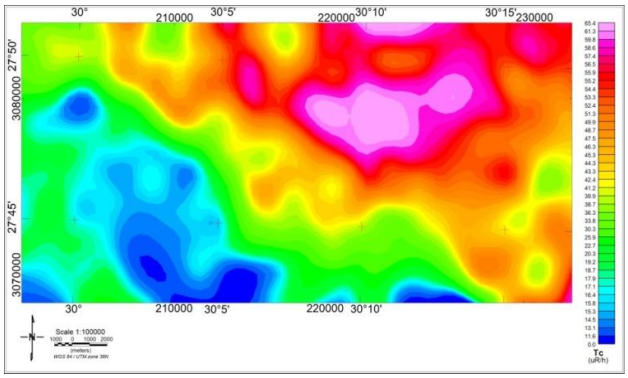

Fig. (5): Map of the Total-Count Radiometric Data, West Mallawi Area, Central Western Desert, Egypt.

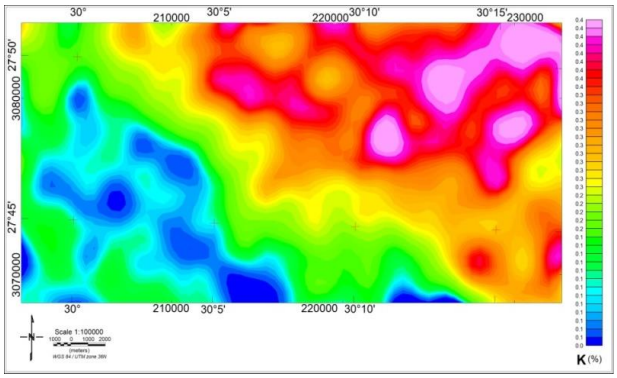

Fig. (6): Map of the Potassium Concentration, West Mallawi Area, Central Western Desert, Egypt.

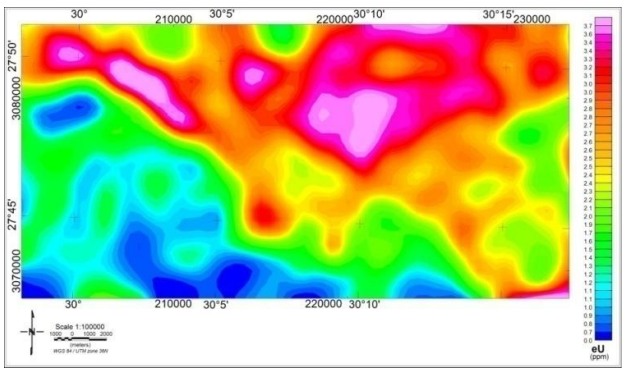

Fig. (7): Map of the Equivalent Uranium Concentration, West Mallawi Area, Central Western Desert, Egypt.

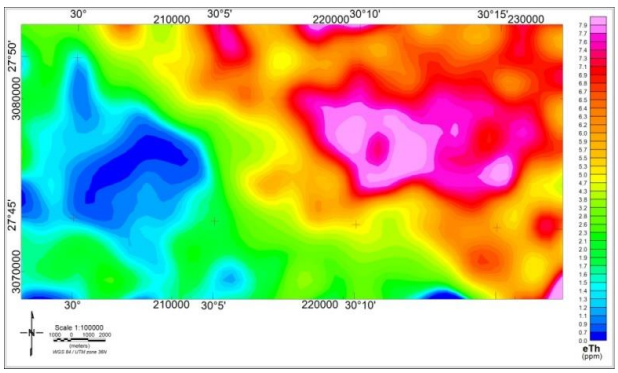

Fig. (8): Map of the Equivalent Thorium Concentration, West Mallawi Area, Central Western Desert, Egypt.

In the Total count map, there are three major levels of radiation, the lowest level is ranging from five to 14 µR/h and this range is represented with the deep and pale blue color. This range is mainly correlated with the Abu Muharik Formation, that occupies the southwestern part of the study area. The intermediate level (18 - 40µR/h) is represented by the green color. This range is correlated with the Mokattam Group that cover the southern portion of the study area. The highest level (55 - 65µR/h) is represented by the yellow, orange, red and magenta colors. This range is encountered in the northeast central part of the study area.

on the potassium map (Fig. 6) there are three major levels of radiation. The lowest level is ranging from zero to 0.1 %, and this range is represented with the deep and pale blue color. This range is mainly correlated with the Abu Muharik Formation that occupies the south western part of the study area. The intermediate level (0.1- 0.3%) is represented with the green color. This range is correlated with the Mokattam Group that cover the southern portion of the study area. The highest level (0.3 - 0.4%) is represented by the yellow, orange, red and magenta colors. This range is encountered in the northeastern corner of the study area.

on the uranium map (Fig. 7) there are three major levels of radiation. The lowest level is ranging from 0 to 1.2 ppm and this range is represented with the deep and pale blue color. This range is mainly correlated with the Abu Muharik Formation, that occupies the south western part of the area. The intermediate level (1.5 - 2.3ppm) is represented with the green color. This range is correlated with the Mokattam Group covering the southern portion of the study area. The highest level (3 - 5.2ppm) is represented by the yellow, orange, red and magenta colors. This range is correlated with the Gebel Qatrani Formation deposits that encountered in the northwestern corner of the study area.

In the thorium map (Fig. 8), there are three major levels of radiation, the lowest level is ranging from zero to 1.5 ppm and this range is represented with the deep and pale blue color. This range is mainly correlated with the Abu Muharik Formation, occupying the south-western part of the area. The intermediate level is (2 - 4 ppm) is represented by the green color. This range is correlated with the Mokattam Group the covering southern portion of the study area. The high level (7 - 9ppm) is represented by the yellow, orange, red and magenta colors. This range is encountered in the northeast central part of the study area.

GENERATION AND DESCRIPTION OF THE RADIOELEMENTS COMPOSITE IMAGES

Airborne spectral radiometric surveying of the study area provided valuable information from the four parameters (variables) namely: total-count of the gamma radiation (TC, in µR/h) absolute concentrations of the three radioelements: potassium (K, in %) equivalent uranium (eU, in ppm) and equivalent thorium (eTh, in ppm). In addition to these four measured variables (Figs. 9, 10, 11 & 12), four composite colour images were also produced according to the following variable combinations:

1. **The radioelement composite image** (Fig. 9) combines the data for eU (in green) eTh (in blue), and K (in red) and provides on one display an overall picture of the radioelement distributions in the study area. This image offers much in terms of lithologic discrimination based on color differences. The high-level radiation (bright areas) is encountered mostly in the northeastern parts of the area.
2. **The potassium composite image** (Fig. 10) combines K (in red) with its two ratios K/eU (in green) and K/eTh (in blue). This image shows the overall spatial distribution of the relative potassium concentration. It also highlights areas associated with potassium enrichment zones. These alteration zones are frequently associated with the formation of various types of non-radioactive mineral deposits. The color zones displayed on the potassium composite image provided a good discrimination for the various geologically mapped lithologies and lithofacies changes previously interpreted from the radioelement, uranium and thorium color composite images. An attempt was made to relate the spatial distribution of the known occurrences of mineral deposits in the study area with the spatial variations in the relative concentration of potassium (Fig. 10). This attempt revealed some significant correlation which suggests that this potassium enrichment is associated with the formation of these mineral deposits and may provide an exploration guide for these deposits in this geologic environment. The high-level concentration (bright area) is encountered in the northeastern corner of the study area.
3. **The uranium composite image** (Fig. 11) combines eU (in red) with its two ratios eU/eTh (in blue) and eU/K (in green). The relative concentration of uranium with respect to both potassium and thorium is an important diagnostic factor in the recognition of possible uranium deposits (IAEA 1988). Uranium enrichment in specific circumstances provides a sensitive pointer to many non-radioactive mineral deposits, e.g. gold and copper deposits. The uranium composite image also reflects lithologic differences and could be useful in geologic mapping problems (Duval, 1983). The high level concentration (bright area) is encountered in the northwest corner and southern central parts of the study area, and would extend further through the southern border.

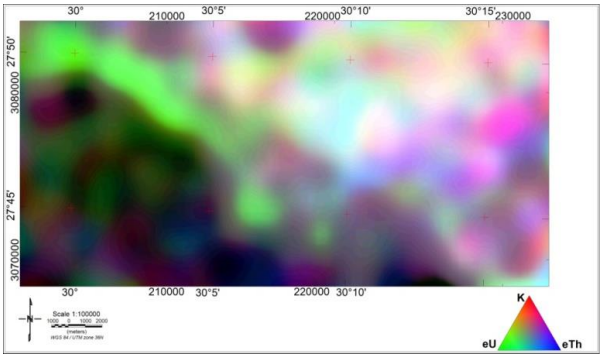

Fig. (9): Radioelement Composite Image, West Mallawi Area, Central Western Desert, Egypt.

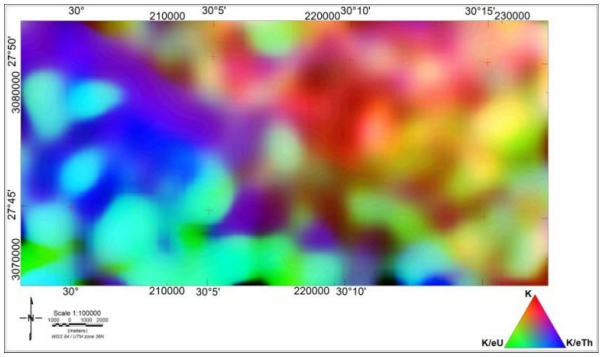

Fig. (10): Potassium Composite Image, West Mallawi Area, Central Western Desert, Egypt.

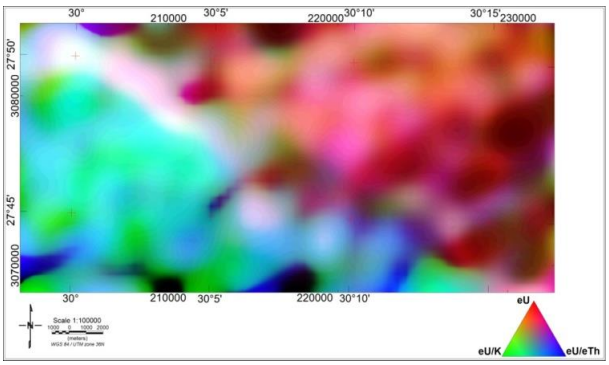

Fig. (11): False-Color Uranium Composite Image, West Mallawi Area, Central Western Desert, Egypt.

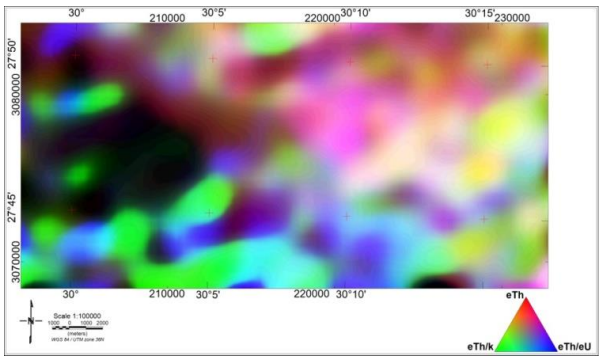

Fig. (12): False-Color Thorium Composite Image, West Mallawi Area, Central Western Desert, Egypt.

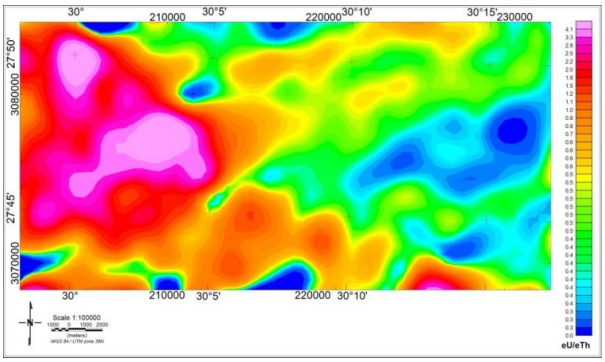

Fig. (13): Radioelement Leads, of the West Mallawi Area, Central Western Desert, Egypt.

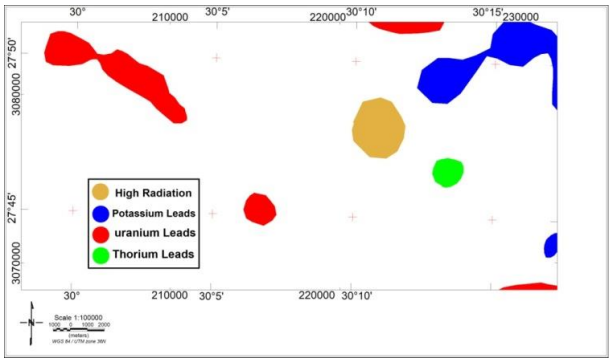

Fig. (14): Map of the Uranium to Thorium Ratio Values, West Mallawi Area, Central Western Desert, Egypt.

4. **The thorium composite color image** (Fig. 12) combines eTh (in red) with its two ratios eTh/eU (in blue) and eTh/K (in green). This image emphasizes the relative distribution of thorium and highlight areas of thorium enrichment. The thorium image helps the geologic mapping and offers a good color discrimination of lithologic differences and lithofacies changes (Duval et al 1983). The high level concentration (bright area) is presented in the southeast near the central part of the study area.

The brightest places were determined from the composite images and grouped into one map which is the Radioelement Leads Map (Fig. 13).

IDENTIFICATION OF RADIOELEMENTS LEADS

As it has been mentioned before, the K, eU and eTh leads are distributed in the radioelement leads map (Fig. 13) as follow;

Potassium leads: Denoted as blue color in the Radioelement Leads Map (Fig. 13). The potassium

leads have been produced from K composite image (Fig. 10). Potassium (K) leads are correlated to potential alterations in the study area. It is encountered in G.Qatrani (Toq) Formation. This formation is located at the northeastern corner of the study area, which is characterized by continental to littoral marine alternating clastics, silt stone, and reddish clay stone.

Uranium Leads: The composite uranium image (Fig. 11) could provide useful information regarding the identification of anomalous zones of enriched uranium concentration. These zones, displayed as bright areas on the Uranium composite image (Fig. 11) those areas are having high values in all three data sets (eU, eU/K, eU/eTh). These Uranium leads are denoted in the radioelement leads map as red color (Fig. 13). The majority of them are located in the northwestern corner of the area in between Gabel Qatrani and Abu Muharik formations, which is characterized by continental to littoral marine alternating clastics, siltstone, and reddish claystone. The second formation is characterized by littoral claystone and siltymarl with Nummulites and white limestone. The remaining Uranium leads are related to Quaternary Gravel (Qg) Formation, Oligocene to Pleistocene and located at the southeastern corner of the study area.

Thorium leads: The bright color on the composite thorium image (Fig. 12) is a good pointer to areas where thorium has been preferentially enriched relative to potassium and uranium. Thorium leads are denoted by green color in the radioelement leads map (Fig. 13) and are associated with G.Qatrani (Toq) Formation, Oligocene to Pleistocene and is located at the central eastern part of the study area and its surroundings.

This thorium-enriched lead represents a good prospect for heavy mineral placer and rare earth deposits (Duval, 1983).

Most of the radioelement anomalies are linked with the NW-SE direction in the northwestern part of the study area, while the radioelement anomalies of the northeastern part are linked with the NE-SW direction. The radioelement anomalies are highly correlated with the surface geologic map (Fig. 4) and very highly correlated with the false-colour Landsat MSS photomap (Fig. 3).

These all radioelement anomalies need more ground follow up and ground geological and geophysical studies.

DISTRIBUTION OF TWO AND THREE RADIOELEMENT RATIOS IN ROCKS

Sedimentary rocks generally have radioelement content reflecting the parent source rocks. Thus, immature sediments derived from granitic sources may be expected to have quite high radioelement content, but in case of more mature sediments, composed primarily of quartz, they should have very low values.

The most direct application of aerial gamma-ray surveying to mineral exploration is in the search for U and Th deposits. Its use for U exploration has been widely reviewed (See, for example IAEA 1979: Killeen 1979: Ward 1981). The search for Th deposits in mineral beach sands is similar application (de Meijer et al. 1994). In these applications, aerial gamma-ray surveys are used to look for elevated concentrations of the element and methods such as element ratios (e.g. Th/U) can be useful in defining subtle expressions of such deposits. To reduce the disturbing effects and contrast of the image and to enhance subtle variations in elemental concentrations due to lithological changes or alteration processes associated with mineralization; ratio pattern maps (eU/eTh, eU/K and eTh/K) were constructed (Figs. 14, 15 and 16).

The eU/eTh ratio data showed the areas of high eU, depleted eTh, although similar values were found over other areas of the map and may reflect compositional variations in the deposits. Thus a high eU/Th ratio is not a unique alteration signature.

The eU/Th ratio data (Fig. 14) best showed the area of high eU present in the northwestern corner, occupying large part of the Abu Muharik Formation (Tea). There is a small anomaly also in the southeastern part of the area. This zone is located at low topographic area.

The eU/K ratio data (Fig. 15) best showed the area of high eU, depleted K, which appear in the northwest corner and occupies a large part in the Abu Muharik Formation, especially at the boundary between Abu Muharik Formation (Tea) and Gebel Qatrani (Toq). There is a small anomaly also in the southern part in the area, at the boundary between Gebel Qatrani (Toq), Mokattam Group (Tems) and Abu Muharik Formation (Tea). This zone is located also at low topographic area.

The eTh/K ratio data (Fig. 16) best showed the area of high eTh and present in the southern part and occupying the Mokattam Group (Tems). There is another anomaly in the middle eastern part in the area, occupying large part of the Gebel Qatrani (Toq).

Other maps were produced to show the sites of mineralization in the area, such as the (eTh*K)/eU ratio data (Fig. 17) which best showed the areas of high (eTh*K) present in the eastern part and occupying the Gravel Quaternary (Qg) Formation Oligocene to Pleistocene, which is located at the southeastern corner of the study area. Other anomaly are occupying also small part in the Gebel Qatrani (Toq) located at the central north part of the area, the (eU*K)/eTh ratio data (Fig. 18) best showed the area of high (eU*K) present in the northwestern corner and occupy large area in the Abu Muharik Formation, at the boundary between Abu Muharik Formation (Tea) and Gebel Qatrani (Toq). The (eU*eTh)/K ratio data (Fig. 19) best showed the area of high (eU*eTh) that associated with Gebel Qatrani (Toq) formation and located at the central eastern part of the study area.

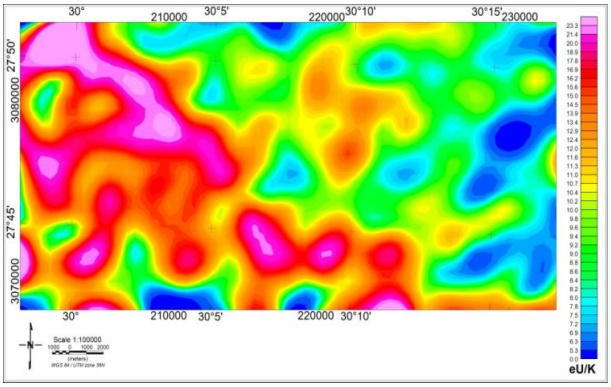

Fig. (15): Map of the Uranium to Potassium Ratio Values, West Mallawi Area, Central Western Desert, Egypt.

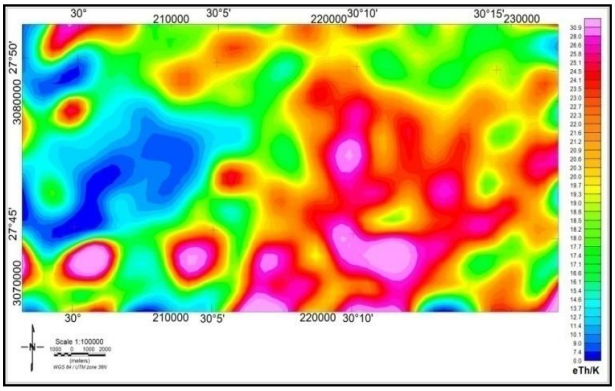

Fig. (16): Map of the Thorium to Potassium Ratio Values, West Mallawi Area, Central Western Desert, Egypt.

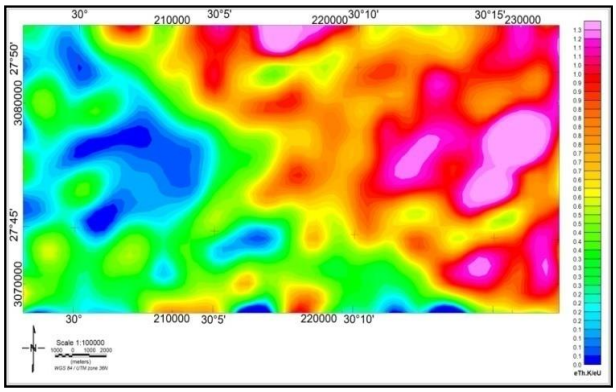

Fig. (17): Map of the (eTh * K) / eU Ratio Values Distribution, West Mallawi Area, Central Western Desert, Egypt.

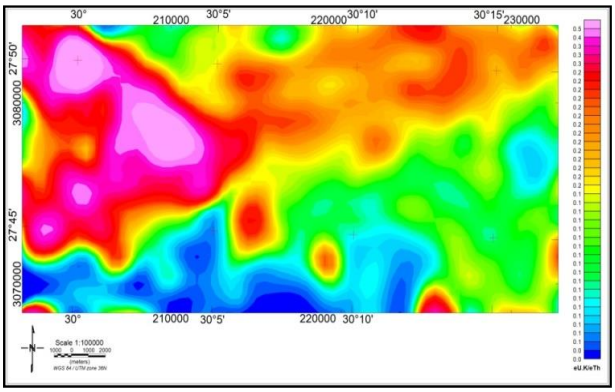

Fig. (18): Map of the (eU * K) / eTh Ratio Values Distribution, West Mallawi Area, Central Western Desert, Egypt.

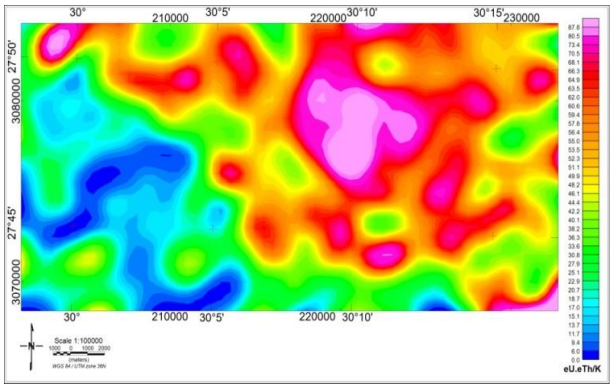

Fig. (19): Map of the (eU * eTh) / K Ratio Values Distribution, West mallawi Area, Central Western Desert, Egypt.

GENERATION AND DESCRIPTION OF THE DISTRIBUTION OF TWO AND THREE RADIOELEMENTS RATIOS COMPOSITE MAPS

The two radioelement ratios composite images (Fig. 20) combines the data for eU/K (in green), eU/eTh (in blue) and eTh/K (in red) and provides on one display an overall picture of the two radioelement ratios distributions in the study area. This image offers much in terms of lithologic discrimination based on color differences. The high-level radiation (bright areas) is encountered in the northeastern central parts of the study area.

The distribution of three radioelement ratios composite image (Fig. 21) combines the data for (eU*K)/eTh (in green), (eU*eTh)/K (in blue) and (eTh*K)/eU (in red) and provides on one display an overall picture of the three radioelement ratios distributions in the study area. This image offers much in terms of lithologic discrimination based on color differences. The high-level radiations (bright areas) are encountered in the northeastern central parts of the study area.

The integrated interpretation among element maps (K, eU, and eTh) radioelement composite map, two and three radioelement composite maps are shown in figures (22 and 23). figure (22) represents the high anomalies, low anomalies, and anomaly leads (K, eU, eTh) figure (23) represents the expected sites of mineralization in the area. It shows that the areas of high (eTh*K) are encountered in both the northern central and the southeastern parts of the study area in green colours. Areas of high (eU*K) are occupying a large part in the northwest and another small area in the southeast in red colour. The large area is related to Abu Muharik Formation (Tea) and Gebel Qatrani (Toq) Formation. The area of high (eU*eTh) is associated with Gebel Qatrani (Toq) Formation and located at the central eastern portion of the study area (Fig. 23) in brown colour.

RADIATION EXPOSURE AND RADIATION DOSE RATES

The Radiation Exposure Rate (RER) map of the study area (Fig. 24) has been calculated from the apparent concentrations of K (%) eU (ppm) and eTh (ppm) by applying the following expression (IAEA, 1991):

Exposure rate (μR/h) = 1.505 K (%) + 0.653eU (ppm) + 0.287eTh (ppm).

The RER map (Fig. 24) shows three main general levels of radiation. The first is a high radiation level oscillates between 4.0 to 6.4μR/h and is associated with magenta color on the RER map. This level was encountered at all of the northeastern portion of the study area (Fig. 24). These high radiation exposure rate areas which represent the first level were correlated with Gebel Qatrani Formation (Toq). The second or intermediate radiation exposure rate (RER) level fluctuates from 1.5 to 3.9μR/h, which vary in color from green and yellow to orange on the RER map (Fig.24). This level is almost occupying the middle of the area of study. This level is correlated with Mokattam Group, Samalut Formation (Tems) and Quaternary Gravel (Qg) deposits in that part. The third or the lowest RER level which varies is from zero to 1.4 μR/h characterized by its blue color. This level was encountered at the southwestern portion of the study area and is correlated with Abu Muharik Formation (Tea) deposits.

The radiation exposure rate (RER) converts directly to Radiation Dose Rate (RDR) through the use of a simple conversion factor as follows (IAEA, 1979):

Dose Rate (mSv/y) = 0.0833 * Exposure Rate (μR/h)

Consequently the (RDR) map of West Mallawi area (Fig. 25), shows certainly the same features of the radiation exposure rate (RER) map (Fig. 25) and consequently the same three main general levels of radiation, but different in values and standard units. The highest radiation dose rate level encountered in the study area ranges from 0.4 to 0.5mSv/y.

Scientists and physicians from international agencies and The International Commission of Radiological Protection (ICRP) has recommended that it is responsible for radiation protection throughout the world have set an annual Radiation Dose-Equivalent (RDE) as follows (IAEA, 2005):

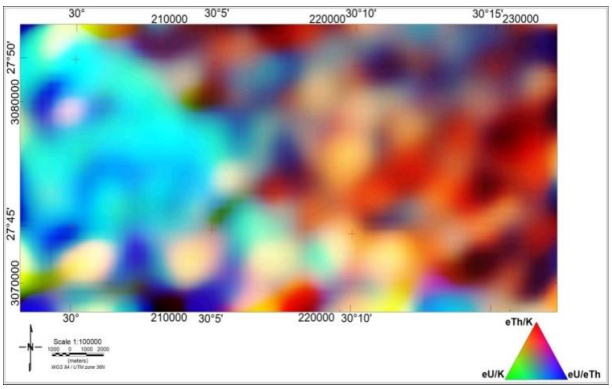

Fig. (20): The Two Radioelement ratios composite image, West Mallawi Area, Central Western Desert, Egypt.

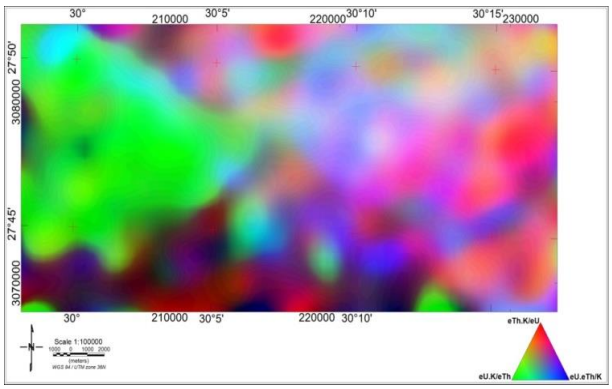

Fig. (21): The three radioelement ratios composite image, West Mallawi Area, Central Western Desert, Egypt.

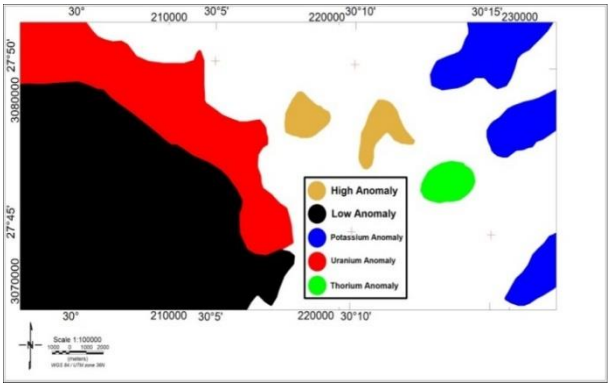

Fig. (22): Integrated interpretation among the element maps (K, eU, and eTh) and radioelement composite image, West Mallawi Area, Central Western Desert, Egypt.

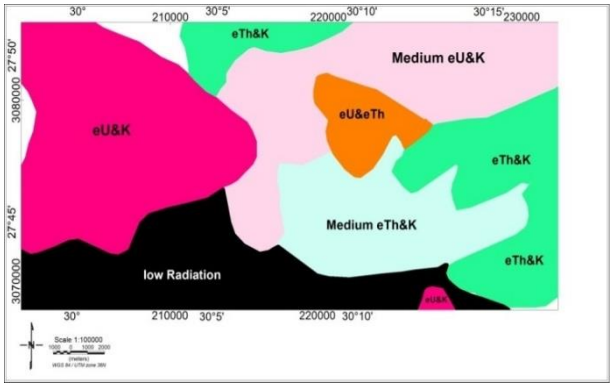

Fig. (23): Integrated interpretation among the two and three Radioelement Ratios composite, West Mallawi Area, Central Western Desert, Egypt.

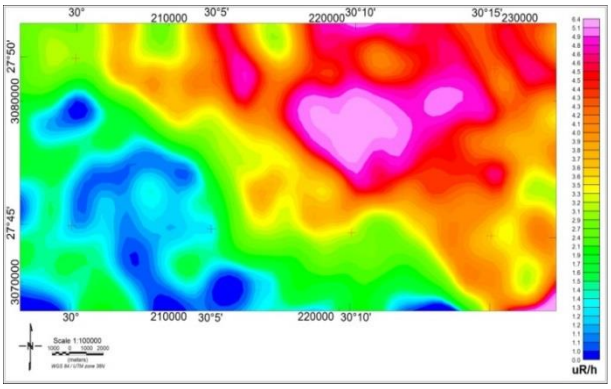

Fig. (24): Map of the Calculated Exposure Rate, West Mallawi Area, Central Western Desert, Egypt.

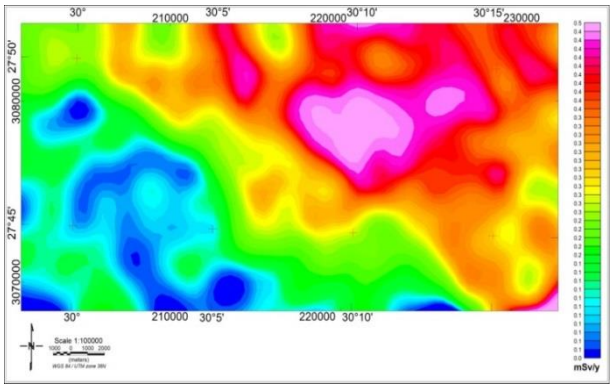

Fig. (25): Map of the Calculated Dose Rate, West Mallawi Area, Central Western Desert, Egypt.

Radiation Dose-Equivalent (RDE) is most unlikely to exceed 1mSv in a year; very little action needs to be taken in this dose range for evaluating and controlling worker doses. If (RDE) ranging between 1 and 6mSv in a year, a dose assessment program is necessary and can utilize work place monitoring or individual monitoring. Wherever (RDE) is likely to exceed 6mSv in a year, individual monitoring of the transport personnel is mandatory (IAEA, 2005).

Concerning the studied area and its surrounding, the mean natural radiation dose rates from the terrestrial gamma-radiation range from 0.0 to 0.5mSv/y. The values between (0 -1mSv/y) remain in the safe side and within the maximum permissible safe radiation dose rate without harm to the individual, with continuous external irradiation of the whole body. The values between (1-1.5mSv/y) should be subjected for further follow up investigation.

CONCLUSIONS

The west Mallawi area is located in Central Western Desert of Egypt. It is located on the western side of the west Nile River. The study area is covered by various sedimentary rocks range in age from Late Cretaceous (Campanian) to Eocene.

The major structural trend that could be traced from all the spectrometric maps is the NW-SE. The lowest radiometric level encountered is related to Abu Muharik Formation. Abu Muharik Formation is located in the southwestern part of the study area. This level has values ranging between zero to17 µR/h in TC, zero to 1.2 ppm in eU, zero to1.5ppm in eTh, and zero to 0.1% in K. The highest level of radiation was found in the northeastern part and related to Gebel Qatrani Formation where the radiation has values ranging between 55 to 65 µR/h in TC, 3 to 5.2 ppm in eU, 7 to 9 ppm in eTh and0.3 to 0.4 % in K. The radioelement composite image showed that the high radiation level (bright areas) is encountered in the northeastern area.

In the northwestern area, most of the radioelement anomalies are oriented towards NW-SE. While in the northeastern area, the radioelement anomalies are oriented towards NE-SW. The radioelement anomalies are highly correlated with surface geology.

The eU/eTh ratio data best showed the area of high eU, which present in the northwestern corner and occupying large part of Abu Muharik Formation (Tea). There is a small part found also in the southeast.

The eU/K ratio data best showed the area of high eU and depleted K, which present in the northwestern corner and occupying large part of Abu Muharik Formation.

The eTh/K ratio data best showed the area of high eTh, which found in the southern part and occupying the Mokattam Group (Tems). Another high anomaly is occupying a large part of Gebel Qatrani Formation (Toq).

Other maps were made to show the sites of mineralization in the area, such as the (eTh*K)/eU ratio data best showed the area of high (eTh*K), the (eU*K)/eTh ratio data best showed the area of high (eU*K) and the (eU*eTh)/K ratio data best showed the area of high (eU*eTh).

The distribution of two radioelement ratios and three radioelement ratio composite images showed that the high-level radiation is encountered in the northeastern central parts of the study area.

Concerning the study area and its surrounding, the mean natural radiation dose rates from the terrestrial gamma-radiation range from 0.0 to 0.5 mSv/y. The values between (0-1 mSv/y) remains in the safe range and within the permissible safe radiation dose rate without harm to the individuals, with continuous external irradiation of the whole body. The values between (1-1.5 mSv/y) should be subjected for further follow up investigation.

REFERENCES

Atlas of Egypt, 1992: Scale 1:250,000. Remote Sensing Centre, Acad. of Sc. Res. and Tech., Cairo, Egypt, V. II.

Charbonneau, B.W., Killeen, P.G., Carson J.M., Cameron, G.W. and Richardson, K.A., 1976: Significance of radioelements concentration measurements made by airborne gamma-ray spectrometry over the Canadian Shield. In Exploration for Uranium Ore Deposits: International Atomic Energy Agency (IAEA), Vienna, Austria, p. 35-53.

Conoco, 1987: Geological Map of Egypt, NF-36 NE Berince, Scale 1: 500,000. Geological survey of Egypt.

De Meijer, R.J., Tanczon, L.C. & Stapel, C., 1994: Radio-metric techniques in heavy mineral exploration and exploitation. Exploration & mining Geology, 3. 389 - 398.

Duval, J.S., 1983: Composite color images of aerial gamma-ray spectrometric data. Geophysics, 48/6, 722-735.

Egyptian Remote Sensing Centre, Egypt (ERSC), 1992: The false-color Land-sat satellite Multispectral Scanner (MSS) image sheets Nos., NF36O and NF36P, scale 1:250,000.

Geosoft Inc., 2010: Geosoft mapping and processing system. Geosoft Inc., Toronto, Canada.

International Atomic Energy Agency "IAEA", 1988: Geochemical exploration for uranium. Technical Reports Series No. 284, Vienna, Austria, 96 p.

International Atomic Energy Agency "IAEA", 1979: Gamma-ray surveys in uranium exploration. Technical Reports Series No. 186, Vienna, Austria.

International Atomic Energy Agency "IAEA", 1991: Airborne gamma-ray spectrometer survey. Technical Reports Series No. 323, Vienna, Austria, 97 p.

International Atomic Energy Agency "IAEA", 1995: Application of uranium exploration data and technique in environmental studies, TECDOC 827, Vienna, Austria.

International Atomic Energy Agency (IAEA), 2005: Decommissioning of Nuclear Facilities, IAEA safety standard series, 27 p.

Killeen, P.G., 1979: Gamma-ray spectrometric methods in uranium exploration —application and interpretation. In: Hood, P.J. (editor), Geophysics and geochemistry in the search for metallic ores. Geological survey of Canada Economic Geology Report 31, 163-229.

Ward, S.H., 1981: Gamma-ray spectrometry in geologic mapping and uranium exploration. Economic geology, 75th Anniversary volume, 840-849.